Electronic Supplementary Information

A Self-Amplifying Nanodrug to Manipulate Janus-Faced Nature of Ferroptosis for Tumor Therapy

Mengzhu Zhang, Xiaohan Qin, Zhipeng Zhao, Qian Du, Qian Li, Yue Jiang, Yuxia Luan*

NMPA Key Laboratory for Technology Research and Evaluation of Drug Products, Key Laboratory of Chemical Biology (Ministry of Education), School of Pharmaceutical Sciences, Cheeloo College of Medicine, Shandong University, Jinan, Shandong, 250012, China, E-mail: yuxialuan@sdu.edu.cn.

Corresponding Author

* E-mail: yuxialuan@sdu.edu.cn. Tel: (86) 531-88382007. Fax: (86) 531-88382548.

Experimental section

Materials

Roscovitine (purity, 100%) was obtained from Topscience Co., Ltd. Methylene blue (MB, purity, 90%) was purchased from Aladdin Industrial Corporation. Alexa Fluor 488-labeled goat anti-rabbit IgG, BCA protein assay kit, HMGB1 rabbit monoclonal antibody (mAb), CRT rabbit monoclonal antibody, COX-2 rabbit monoclonal antibody, PD-L1 rabbit polyclonal antibody, SLC3A2 rabbit polyclonal antibody, glutathione peroxidase assay kit, and lipid peroxidation MDA assay kit were supplied by Beyotime Biotechnology Co., Ltd. IFN-γ and anti-mouse antibodies (PE-labeled PD-L1, FITC-labeled CD11c, FITC-labeled CD8a, APC-labeled CD80, PE-labeled CD86, APC-labeled CD62L, PE-labeled CD3, PerCP-labeled CD44, and APC-labeled CD3) were supplied by BioLegend, Inc. (USA). Horseradish peroxidase (HRP)-labeled goat anti-rabbit monoclonal antibody, GAPDH mouse monoclonal antibody, Horseradish peroxidase (HRP)-labeled goat anti-mouse monoclonal antibody were supplied by Affinity Biosciences Biotechnology Co., Ltd. Hemin (purity□95%), celecoxib (purity□98%), vitamin E (VE, purity□98%), Triton X-100, 3-(4,5-Dimethyl-2-thiazolyl)-2,5-diphenyl-2-H-tetrazolium bromide (MTT, purity≧98%), and 6-Diamidino-2-phenylindole dihydrochloride (DAPI) were obtained from Dalian Meilun Biological Technology Co., Ltd. ELISA kits for PGE_2, TNF-α, IL-2 and IFN-γ were purchased from Multisciences Biotechnology Co., Ltd. Micro reduced Glutathione (GSH) assay kit, glutathione (GSH, purity□98%) and anti-SLC7A11 polyclonal antibody were obtained from Beijing Solarbio Science & Technology Co., Ltd. Albumin human (HSA≧96%) and 2',7'-dichlorofluorescein diacetate (DCFH-DA, purity≧97%) were supplied by Sigma-Aldrich, Inc. Chlorin e6 (Ce6, purity, 93 to 98%) was

purchased from Beijing J & K Technology Co., Ltd. 3,3′,5,5′-tetramethyl benzidine (TMB, purity, 99%) was bought from Shanghai yuanye Bio-Technology Co., Ltd. Dimethyl sulfoxide (DMSO, purity, AR) was purchased from Sinopharm Chemical Reagent Co., Ltd. Ferrostatin-1 (Fer-1, purity□98%) and erastin (purity□98%) were obtained from Glpbio Technology Inc (Montclair, CA, USA).

Preparation of RCH NPs

Celecoxib, roscovitine, and hemin were used to prepare RCH NPs by co-assembling with the assistance of HSA. Typically, celecoxib, roscovitine and hemin were firstly dispersed in 350 μL of dimethyl sulfoxide (DMSO) to form a mixture solution. Then 350 μL of DMSO (containing 2.5 mg of celecoxib, 1.5 mg of roscovitine and 2.5 mg of hemin) was slowly added into HSA (5 mg mL^{-1}) aqueous solution under stirring. To enable the complete co-assembling, the solution was stirred in the dark for 60 min. Then, the solution was dialyzed against water, and the RCH NPs product was achieved by filtering with a 0.80 μm membrane. Ce6-loaded RCH NPs was also prepared according to the similar route.

Characterization of RCH NPs

UV-Vis spectrum of celecoxib, roscovitine, hemin, and RCH NPs was recorded via a UV-Vis spectrophotometer (UV-8000S, Metash). Morphological characterization of RCH NPs was visualized via transmission electron microscopy (TEM, JEM-200CX). The size distribution and zeta potential of RCH NPs were determined by the dynamic light scattering (DLS, Zetasizer Nano ZS90). The stability of RCH NPs was investigated by the change of size distribution at different time at 4 °C.

In vitro release behavior of RCH NPs

The RCH NPs was put into a dialysis bag (MWCO: 1000 Da), then incubated with buffers of different pH (pH 5.0, 6.5 or 7.4), and shaken at a constant speed in a 37 °C constant temperature water bath. At a predetermined time, the dialysis medium was collected and the same volume of fresh medium was added. Finally, the amount of drug release was measured by high performance liquid chromatography (HPLC).

Fenton catalytic activity test

The ability of •OH production of RCH NPs via Fenton reaction was evaluated by the degradation of MB because MB could react with •OH. Firstly, RCH NPs was co-incubated with MB to establish an adsorption/desorption equilibrium. Then the Fenton reaction was conducted in acetic acid buffer solution of different pH (5.0, 6.5, 7.4) at 37 °C with or without H_2O_2. Samples were recovered at predetermined time and measured the absorption intensity at 660 nm to assess the residual amount of MB.

The typical oxidation reaction of TMB (3,3′,5,5′-tetramethyl benzidine) was utilized to further prove the Fenton activity of RCH NPs. Measurements were carried out in acetic acid buffer solution (pH 5.0) containing RCH NPs, TMB and H_2O_2 at 37 °C. The absorbance at 655 nm at the scheduled time was measured by the UV-Vis spectrophotometer.

Cell culture

B16F10 melanoma cells were cultured in RMPI 1640 medium with fetal bovine serum (FBS, 10%) and 1% antibiotics (penicillin-streptomycin, 10 000 U mL^{-1}). Cells were incubated at 37 °C with 5.0% CO_2.

Cellular uptake in vitro

The components in RCH NPs had no efficient fluorescence property, Ce6, as fluorescent marker, was utilized to label the nanoparticles. RCH-Ce6 NPs was prepared in the similar method as that of RCH NPs. Cellular uptake behavior of RCH-Ce6 NPs was evaluated by flow cytometry and laser scanning confocal microscope (LSCM). The B16F10 cells in 6-well plates with 2×10^5 cells/well were cultured. After an overnight incubation, the media were replaced with fresh media containing RCH-Ce6 NPs and free Ce6 to incubate cells. The Ce6 concentration was fixed at 20 μg mL^{-1}. The cells were then washed thrice with PBS and collected by centrifuging. After this, the cells were resuspended with PBS for analysis via flow cytometry. The time dependence of uptake was quantitatively measured by flow cytometry. For achieving fluorescent images, cells were fixed by paraformaldehyde (4%) for 10 min, and then were stained for 10 min with DAPI for characterization by LSCM.

Cellular •OH generation

DCFH-DA, as probe, was used to measure the •OH production ability of RCH NPs via flow cytometry and fluorescent inverted microscope. In brief, the B16F10 cells in 6-well plates (2×10^5 cells/well) were kept overnight and then treated with fresh media containing free hemin and RCH NPs for 12 h. The hemin concentration was fixed at 20 μg mL^{-1}. The cells were subsequently washed and cultured with 20 μM DCFH-DA for another 20 min. The cells were finally washed thrice by PBS, collected and resuspended for flow analysis, or captured by fluorescence microscopy for fluorescent images.

Cytotoxicity assay in vitro

The cytotoxicity of hemin, celecoxib, roscovitine, and RCH NPs at different concentrations was conducted on B16F10 cells via MTT assay. Typically, B16F10 cells were cultured

overnight in 96-well plates with 6000 cells/well in 200 μL medium. Subsequently, the treatments of cells were performed by fresh medium containing hemin, celecoxib, roscovitine and RCH NPs, respectively. The concentrations of hemin, celecoxib and roscovitine varied from 5.00 to 30.00 μg mL^{-1} for hemin, 1.41 to 8.46 μg·mL^{-1} for roscovitine and from 4.00 to 24.00 μg mL^{-1} for celecoxib. After 24 h incubation, 10 μL MTT solution (5 mg mL^{-1}) was put in and the cells were incubated for another 4 h. Hereafter, the supernatant was substituted by the DMSO to dissolve blue formazan crystal. The absorbance of the well at 490 nm was measured through microplate reader. The cell inhibition ratio was determined by the following formula:

$$\text{Cell inhibition ratio (\%)} = \frac{A_{positive} - A_{sample}}{A_{positive} - A_{blank}} \times 100\% \quad (1)$$

Here medium without drugs or cells acted as the blank group, and cells with only medium were regarded as the positive group. The experiment was tested in parallel three times.

Furthermore, the standard ferroptosis inhibitors were employed to test the contribution of ferroptosis to the RCH NPs-induced cytotoxicity in B16F10 cells. The ferroptosis-related cytotoxicity of RCH NPs (dose of hemin varied from 5.00 to 30.00 μg mL^{-1}) was investigated by the co-supplement of RCH NPs with various ferroptosis inhibitors such as 50 nM Fer-1, 100 μM VE, and 5 mM GSH. Cell inhibition ratio was investigated via using the same MTT method.

HMGB1 release in vitro

Immunofluorescence was utilized to evaluate the HMGB1 release induced by RCH NPs. B16F10 cells were cultured with celecoxib, roscovitine, hemin, and RCH NPs for 24 h. Then, the cells were washed by PBS at three times and then were fixed by paraformaldehyde (4%) for

10 min. After treatment with 0.1% Triton X-100 for 10 min, the cells were cultured with the HMGB1 rabbit mAb, and labeled with Alexa Fluor 488-labeled goat anti-rabbit IgG successively. After labeled with DAPI for 5 min, the samples were imaged with LSCM. Cells with no drug treatment were considered as the control group.

CRT exposure in vitro

Immunofluorescence was utilized to evaluate the CRT exposure induced by RCH NPs. B16F10 cells with 2×10^5 cells/well were seeded in the 6-well plates and incubated with celecoxib, roscovitine, hemin and RCH NPs for 24 h. Afterwards, cells fixed by 4% paraformaldehyde for 10 min, were successively stained with the CRT rabbit mAb, Alexa Fluor 488-labeled goat anti-rabbit IgG and DAPI for analyzing by LSCM. The cells with no addition of drug were considered as the control group.

ATP secretion in vitro

ATP analysis kit was utilized to evaluate the secretion of ATP induced by RCH NPs. B16F10 cells with 2×10^5 cells/well were seeded in the 6-well plates and incubated with celecoxib, roscovitine, hemin and RCH NPs. Then, the cells were processed according to the instruction of the ATP analysis kit to collect samples, followed detected by microplate reader.

BMDCs activation and maturation in vitro

Bone-marrow-derived dendritic cells (BMDCs) were obtained from bone marrow of healthy C57BL/6 mice. To study DCs activation and maturation in vitro, the B16F10 cells experienced pretreatment with celecoxib, roscovitine, hemin and RCH NPs for 24 h, and were co-incubated with BMDCs for another 24 h. Then, the recovered BMDCs were stained by APC anti-mouse

CD80, FITC anti-mouse CD11c, and PE anti-mouse CD86 antibodies for analyzing via flow cytometry. Cells with no addition of drug were regarded as the control group.

Evaluation of SLC7A11 and SLC3A2 expression in vitro

LSCM was used to examine the expression levels of SLC7A11 and SLC3A2 in vitro. B16F10 cells were prepared the day prior. The cells experienced the treatment with PBS, RCH NPs, and RCH NPs with IFN-γ added, separately. For qualitative analysis, cells fixed by paraformaldehyde (4%) for 10 min, were successively stained by SLC7A11 rabbit polyclonal antibody/SLC3A2 rabbit polyclonal antibody, Alexa Fluor 488-labeled goat anti-rabbit IgG and DAPI, and then were detected visually by LSCM.

MDA assay in vitro

Changes of MDA content induced by RCH NPs were determined by lipid peroxidation MDA assay kit. The seeded B16F10 cells were conducted in the 10 cm culture dish. With various treatments (PBS, hemin, RCH NPs, RCH NPs+IFN-γ and RCH NPs+Fer-1), the cells were then lysed with a solution of 400 μL cell lysis buffer, followed by centrifuging to obtain supernatant for MDA analysis. Subsequently, BCA protein assay kit was utilized to detect protein concentration of the supernatant for normalizing MDA content.

Assessment of intracellular GSH

Changes of GSH content induced by RCH NPs were determined by the commercial GSH assay kit. The seeded B16F10 cells were conducted in the 10 cm culture dish. With various treatments (PBS, hemin, RCH NPs, RCH NPs+IFN-γ and RCH NPs+Fer-1), the cells were washed by PBS, followed by collection after the trypsin digestion and centrifugation, and then were resuspended by PBS to count for normalization of the GSH content. After centrifugation

again, the cells were re-suspended by cell precipitation reagent, and then freeze-thawed process was repeatedly thrice. The supernatants for the sample in each group were conducted based on manufacturer's protocol upon detecting the content of GSH.

GPX4 activity assay in vitro

Changes of GPX4 activity induced by RCH NPs were determined by cellular glutathione peroxidase assay kit. The seeded B16F10 cells were conducted in the 10 cm culture dish. With various treatments (PBS, hemin, RCH NPs, and RCH NPs+IFN-γ), the cells were then lysed with the solution of 400 μL cell lysis buffer, followed by centrifuging to obtain supernatant for GPX4 activity analysis. BCA protein assay kit was subsequently utilized to detect protein concentration in the supernatant for normalization of the GPX4 activity.

COX-2 activity assay in vitro and in vivo

COX-2 expression levels in the B16F10 cells were assessed via LSCM and western blot. B16F10 cells were seeded in 6-well plates with 2×10^5 cells/well. After incubation overnight, cells were incubated with media containing H@H NPs and RCH NPs for 24 h. Afterwards, cells were washed by PBS, and then fixed by paraformaldehyde (4%), finally labeled by COX-2 rabbit mAb, Alexa Fluor 488-labeled goat anti-rabbit IgG and DAPI in sequence. All samples were analyzed by LSCM. Cells underwent no treatment of drug were used as the control group.

The expression of COX-2 in B16F10 cells under different formulation treatments were also analyzed by western blot. Cells of different groups were treated with 200 μL of RIPA on the ice for 30 min, and centrifugated to obtain the cell lysate as well as boiling at 100 °C for 5 min for denaturation. The cell lysates were conducted for electrophoresis, followed by incubation

of antibody at 4 °C. The developer was added. The blots were characterized by the Bio-Rad ChemiDoc MP gel imaging system. Cells with no treatment of drug were used as the control group. The verification of COX-2 expression at animal level was carried out on tumor-bearing mice with different formulations (NS, H@H NPs, and RCH NPs). After the treatment, COX-2 expression of the tumor tissues was analyzed by immunofluorescence-stained images.

PGE_2 level analysis in vitro

B16F10 cells in the 6-well plates with 2×10^5 cells/well were first incubated with H@H NPs and RCH NPs for 24 h. The amounts of PGE_2 in supernatants were measured using PGE_2 ELISA kit based on instructions of manufacturer. The result was defined as PGE_2 content (%). Cells underwent no treatment of drug were used as the control group.

Verification on enhanced PD-L1 expression by ferroptosis.

Flow cytometry and LSCM were used to detect the PD-L1 expression level in B16F10 cells. The overnight seeded B16F10 cells in 6-well plates were cultured with roscovitine or RCH NPs for 24 h with or without stimulation of IFN-γ, respectively. The concentration of roscovitine was fixed at 5.325 μg mL^{-1}. For qualitative analysis, cells fixed by paraformaldehyde (4%, 10 min), were successively stained with PD-L1 rabbit polyclonal antibody, Alexa Fluor 488-labeled goat anti-rabbit IgG and DAPI, followed with detecting visually via LSCM. For the quantitative assay, the cells were recovered after trypsin digestion and centrifugation, and followed by staining with PE anti-mouse PD-L1 antibody for the flow cytometry analysis. Cells with no drug or IFN-γ treatment were regarded as the control group. The verification of PD-L1 expression at animal level was carried out on tumor-bearing mice experiencing with the treatment of different formulations (NS, H@H NPs, and RCH NPs). After the treatment,

immunofluorescence-stained images of tumor tissues were utilized to investigate the presence of CD8+ T cells and PD-L1 expression.

Hemolysis evaluation

Hemolysis experiment was performed to evaluate the biocompatibility in blood for verifying the feasibility of RCH NPs in intravenous administration with 2% (v/v) red blood cell suspension (RBCS) of rabbit. Typically, various concentrations (5 to 200 μg mL^{-1}) of 150 μL RCH NPs were put in the solution of 1.10 mL saline and 1.25 mL RBCS, respectively. Then, the water (1.25 mL) with RBCS (1.25 mL) was utilized as the positive control. The saline (1.25 mL) with RBCS (1.25 mL) was regarded as the negative control. After 3 h incubation at 37 °C, centrifugation was conducted. the absorbance (540 nm) for the supernatant was evaluated by microplate reader. Each experiment was done by three times. The following equation was utilized for evaluation of hemolysis ratio:

$$\text{Hemolysis ratio (\%)} = \frac{A_{sample} - A_{negative}}{A_{positive} - A_{negative}} \times 100\% \quad (2)$$

Here A_{sample}, $A_{positive}$, $A_{negative}$ corresponded to absorbance of RCH NPs groups, positive control groups and negative control groups.

Animal

C57BL/6 mice (female, 6-8 weeks) were obtained from Jinan Pengyue Laboratory Animal Co., Ltd. All animal experiments were approved by Shandong University Animal Experiment Ethics Review and the Health Guide for the Care and Use of Laboratory Animals of National Institutes. (SYXK(Lu)20190005). All mice received care in accordance with international ethics guidelines.

Fluorescence imaging in vivo

Ce6-incorporated nanodrug was utilized as fluorescent indicator to evaluate the biodistribution of the RCH NPs because RCH NPs lacked effective fluorescence property. Real-time tracking in vivo of RCH NPs was conducted via Ce6-loaded RCH NPs, which was prepared as described above. B16F10 cells resuspended in PBS were injected subcutaneously in C57BL/6 mice with 1×10^6 cells per mouse in the back region of mice. After 7 days, tumor volume in mice reached ~200 mm^3. Then, the mice were injected with RCH-Ce6 NPs or free Ce6 (Ce6: 6 mg kg^{-1}). With live animal in vivo imaging system, optical imaging was conducted on anesthetized mice to acquire the fluorescence signals at predetermined time. At 24 h post injection, mice were sacrificed for dissection to obtain tumors and main organs for imaging.

In vivo antitumor performance

B16F10 cells were subcutaneously injected into back region of the mice with 1×10^6 cells per mouse. When tumor became ~90 mm^3, the mice were therefore divided into 5 groups: normal saline (NS), celecoxib, roscovitine, hemin, and RCH NPs. The treatments performed intravenously every 2 days with celecoxib dose of 7.12 mg kg^{-1}, roscovitine dose of 2.51 mg kg^{-1}, and hemin dose of 8.90 mg kg^{-1}. During treatments, the tumor volumes and body weights were detected. When treatments were finished, mice were therefore sacrificed for dissection to obtain tumors and main organs. Hematoxylin and eosin (H&E) staining analysis of the major organs and the tumors was utilized to evaluate the biosafety and bioactivity. For NS group and RCH NPs group, blood was collected from the eyeball of mouse, then centrifugated to obtain supernatant for determination of ALT and AST content. The below formulas were utilized to determine tumor volume and inhibition ratio:

$$\text{Tumor volume } (mm^3) = \frac{L \times W^2}{2} \quad (3)$$

$$\text{Tumor inhibition ratio } (\%) = \frac{W_0 - W_t}{W_0} \times 100\% \quad (4)$$

Here W and L meant tumors' width and length, respectively; W_0 represented average tumor weight for NS group; W_t represented final tumor weight for the treatment group.

In vivo immune response experiments

After treating, inguinal-draining lymph nodes, tumors, and serum were recovered to understand antitumor immune response. Cytotoxic T cells (CD8+ T cells, stained by APC anti-mouse CD3 antibody and FITC anti-mouse CD8a antibody) in both tumors and spleens were characterized via flow cytometry. The DCs (stained by FITC anti-mouse CD11c antibody, APC anti-mouse CD80 antibody, and PE anti-mouse CD86 antibody) in inguinal-draining lymph nodes were characterized via flow cytometry. Elisa kits were used to characterize IL-2, TNF-α and IFN-γ of serum harvested from treated mice.

The abscopal effect of RCH NPs for bilateral model

Bilateral tumor model experiment was conducted to evaluate the abscopal effect of RCH NPs. B16F10 cells were subcutaneously injected into right back region (as the primary tumor) of the mice with 8×10^5 cells per mouse. Four days after inoculation, the same numbers of B16F10 cells were injected in the other flank (as the abscopal tumor). When volume of primary tumors reached ~60 mm^3, the mice were therefore randomly divided into two groups: NS and RCH NPs. Treatments were conducted by intratumoral (primary tumor) administration every 4 days for 3 times. During treatments, the volumes of primary and abscopal tumors and body weights of mice were detected. The determination of tumor volumes and inhibition ratios were

the same as before. When treatments were finished, mice were therefore sacrificed for dissection to obtain tumors to study the antitumor effect.

Anti-metastasis evaluation

Upon establishing lung metastatic tumor model, the B16F10 cells resuspended in PBS were subcutaneously injected in the mice with 1×10^6 cells per mouse. After the tumor volume became ~90 mm^3, the mice were intravenously administrated with 2.0×10^5 B16F10 cells. After one day, the dividing for groups and the treatment of mice were similar to the antitumor performance study. After 14 days, the mice were sacrificed to strip lungs for counting the metastatic tumor nodules and analyzing H&E staining images.

Long-term immune response evaluation

To examine the immune memory effect of RCH NPs, the B16F10 cells resuspended in PBS were subcutaneously injected in the mice with 1×10^6 cells per mouse. After tumor volume became ~90 mm^3, the groups and the administration of mice were similar to the antitumor performance study. The residual tumors were all resected by surgical operation after the last treatment. At day 16 post the surgical resection, the spleens of the mice were separated for analysis of central memory T cells (T_{CM}, CD3+CD8+CD62L+CD44+) and effector memory T cells (T_{EM}, CD3+CD8+CD62L−CD44+) via flow cytometry. And the mice in the groups of NS and RCH NPs were injected by B16F10 cells via caudal vein at day 16 after surgical resection to further study the recurrence of tumors. At day 15 post the rechallenge of tumor cells, the lungs were obtained for analysis of tumor recurrence.

Statistical analysis

All of the data were defined as mean ± SD. Student's t-test or one-way analysis of variance followed with Turkey's multiple comparisons test was utilized to compare between two groups or multiple groups, respectively. Significant differences were presented by $*p < 0.05$, $**p < 0.01$, and $***p < 0.001$, $****p < 0.0001$.

Supplementary Figures

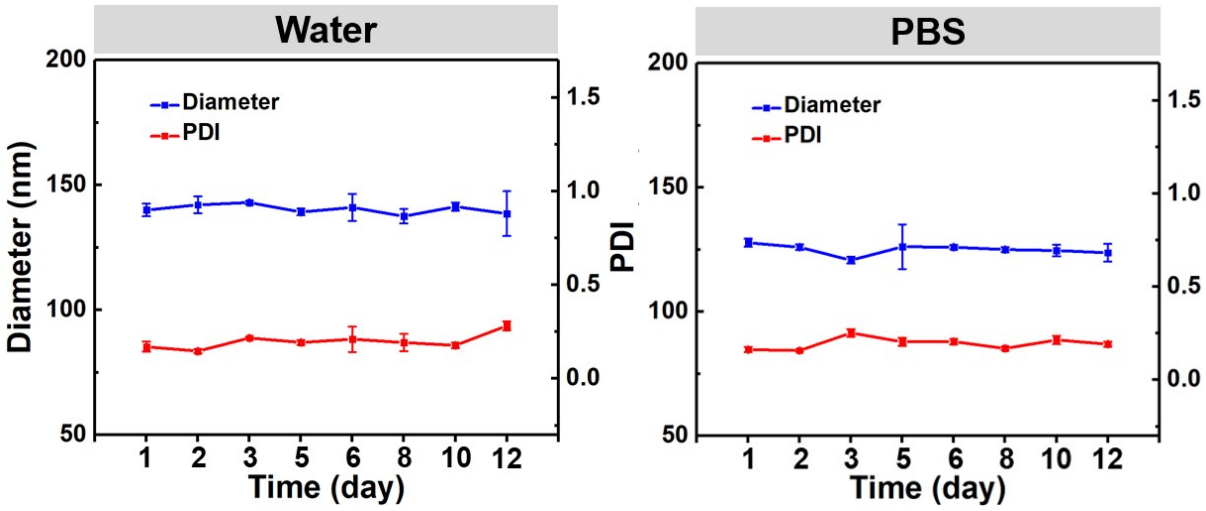

Fig. S1 The particle size of RCH NPs at different time in different media.

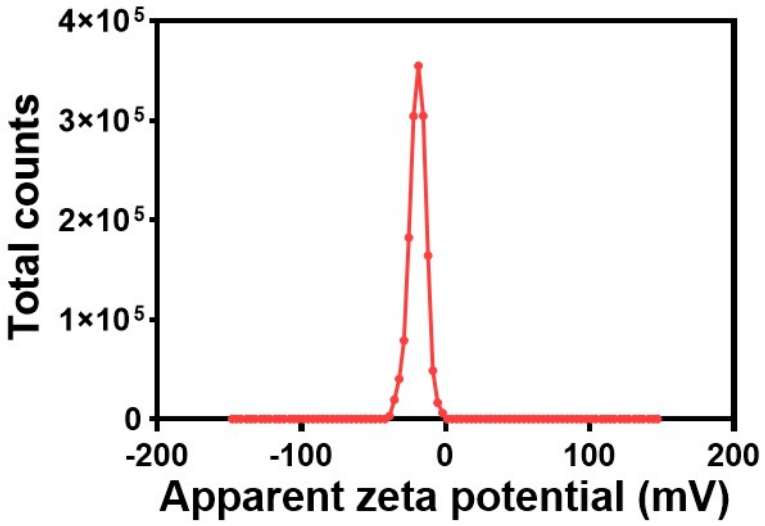

Fig. S2 Zeta potentials of RCH NPs

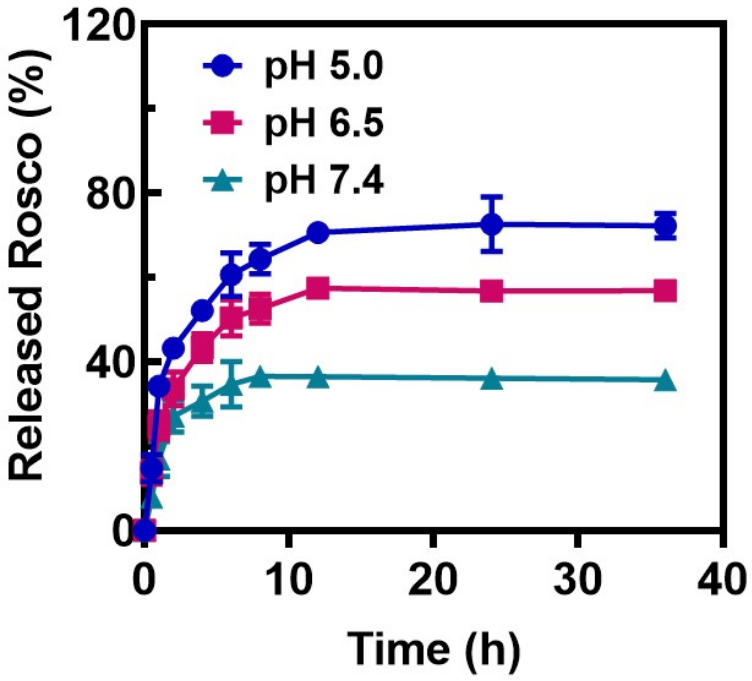

Fig. S3 In vitro release behavior of roscovitine at pH 7.4, 6.5 and 5.0.

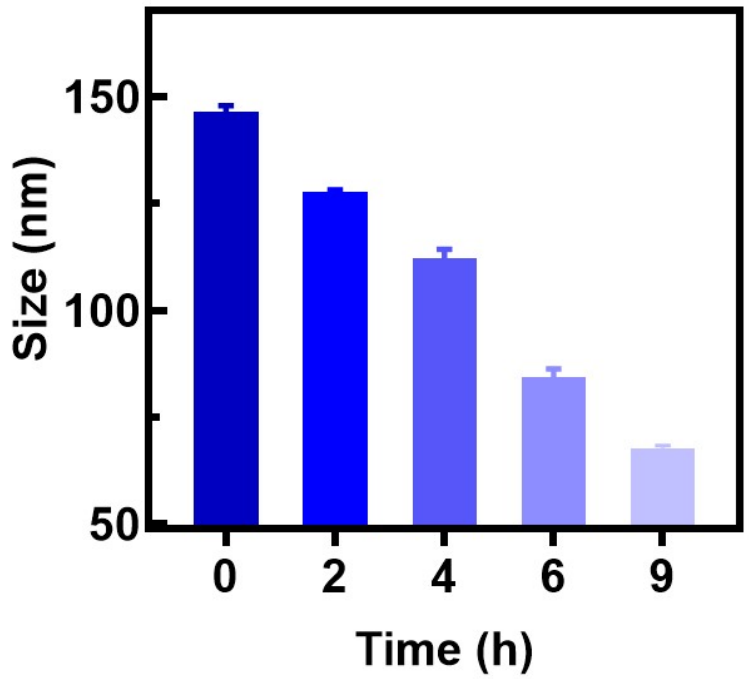

Fig. S4 DLS measurements of RCH NPs after 0, 2, 4, 6 and 9 h of incubation in PBS (pH 5.0).

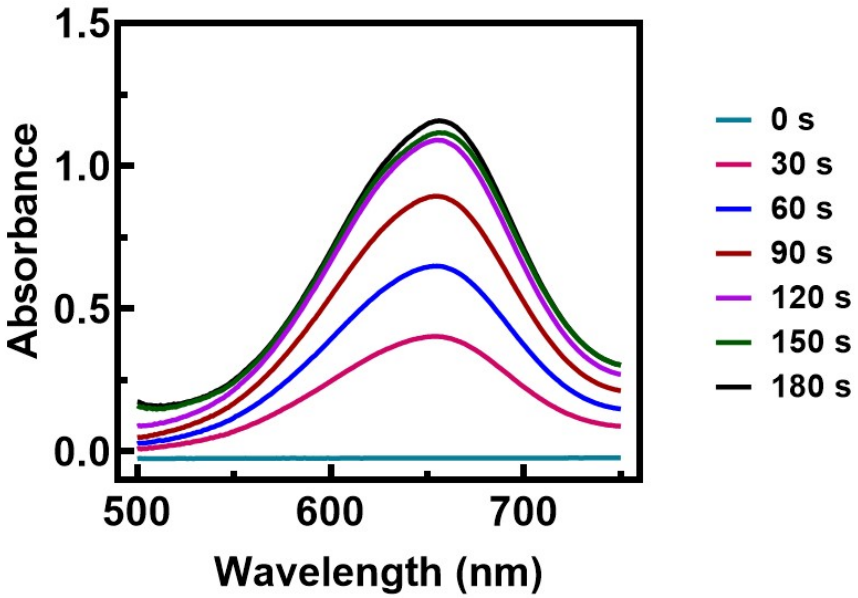

Fig. S5 UV-Vis spectra of the oxTMB.

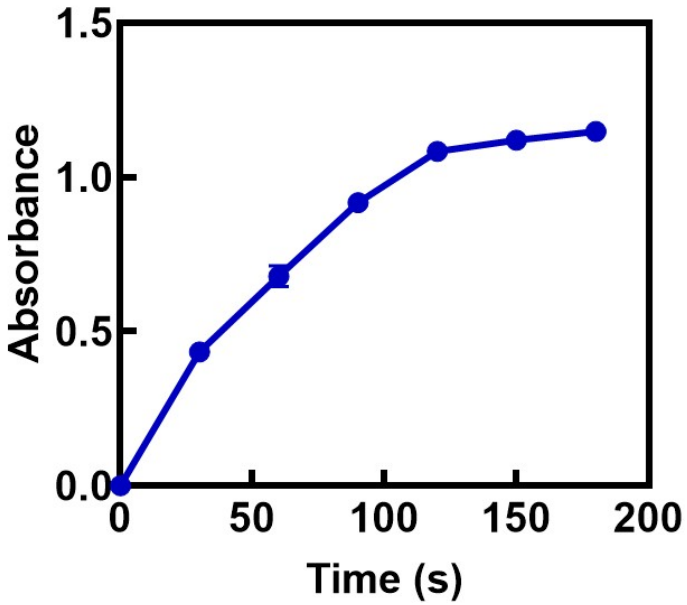

Fig. S6 Absorbance of the oxTMB at 655 nm.

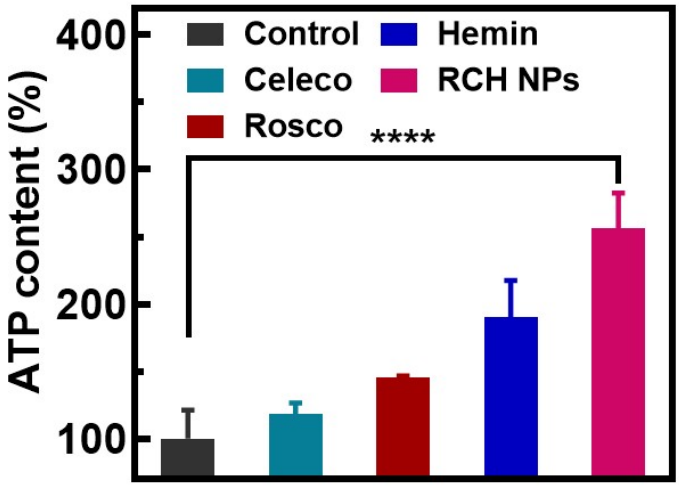

Fig. S7 ATP secretion of B16F10 cells after different treatments.

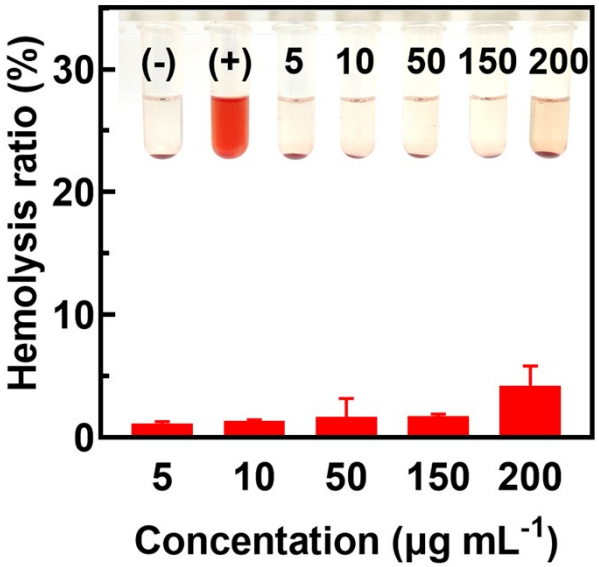

Fig. S8 Hemolysis ratio of RCH NPs at different concentrations (n=3).

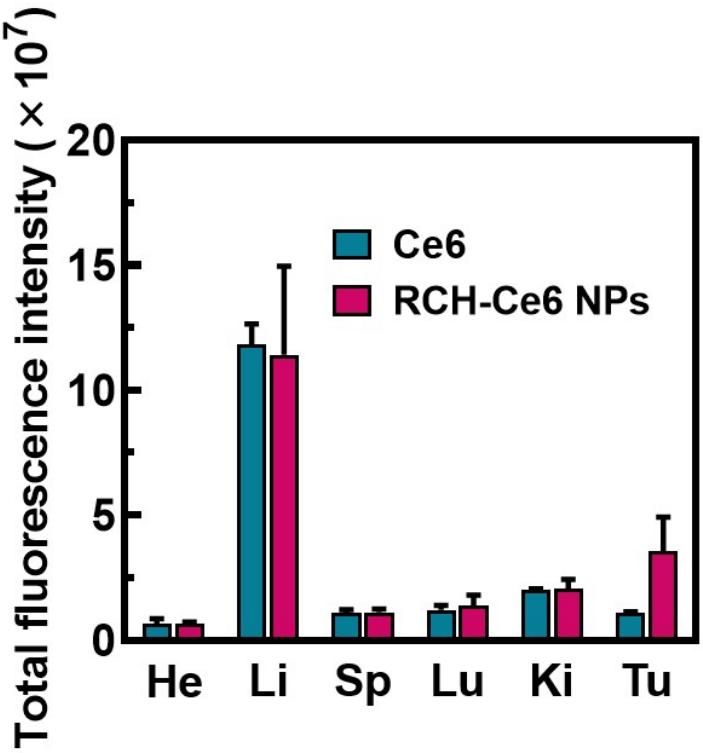

Fig. S9 Total fluorescence intensity of the excised organs and tumors (n=3).

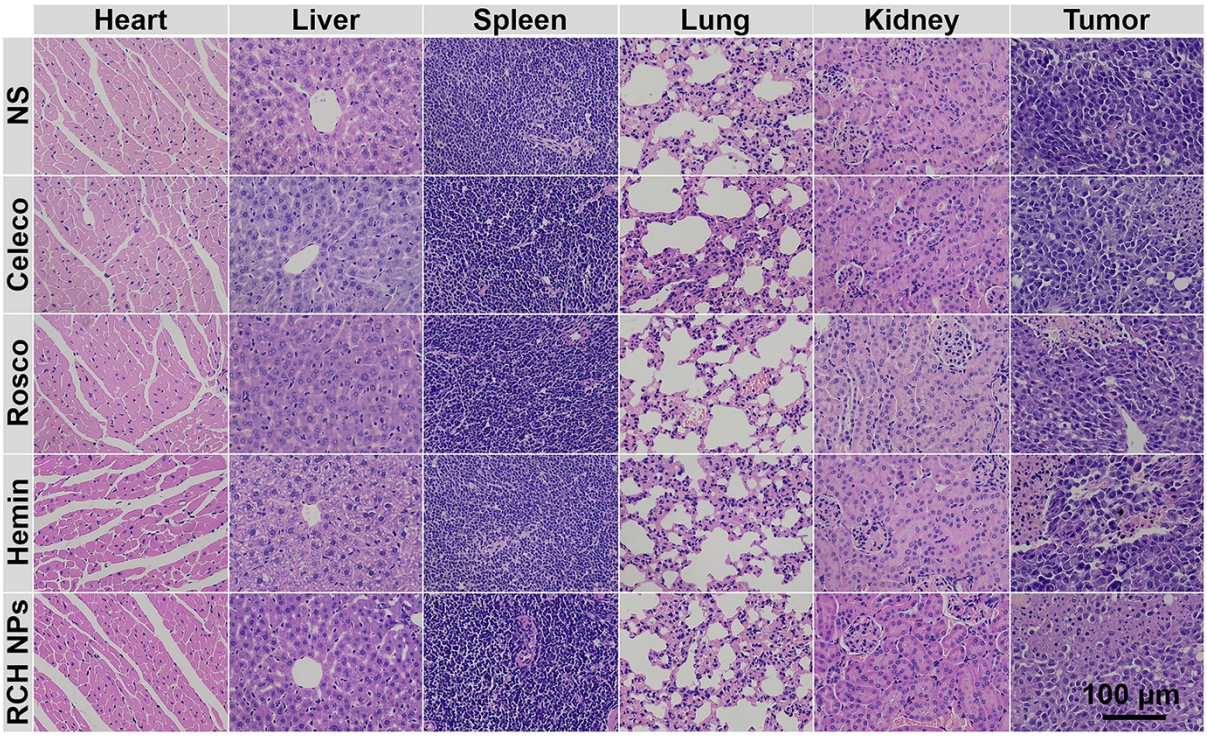

Fig. S10 H&E staining images of main organs and tumors extracted from mice after different treatments.

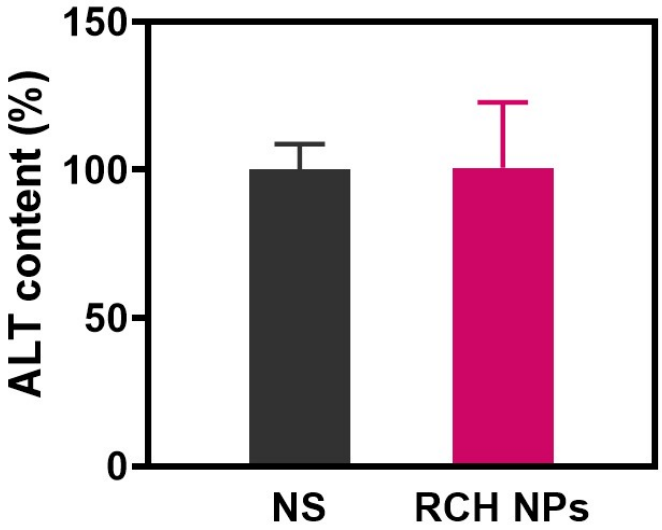

Fig. S11 The measurement of blood biochemical marker for ALT.

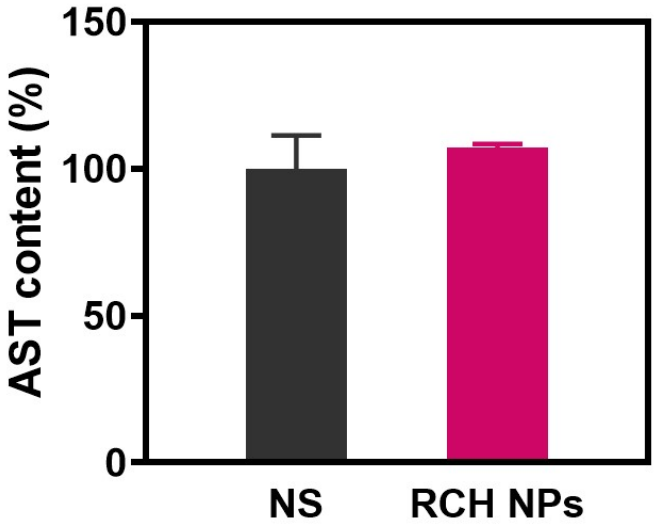

Fig. S12 The measurement of blood biochemical marker for AST.

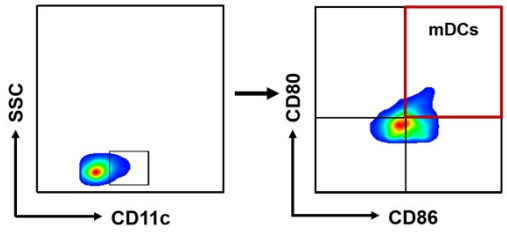

Fig. S13 Gating strategy for flow cytometry analysis of the percentages of maturated DCs in the TDLNs.

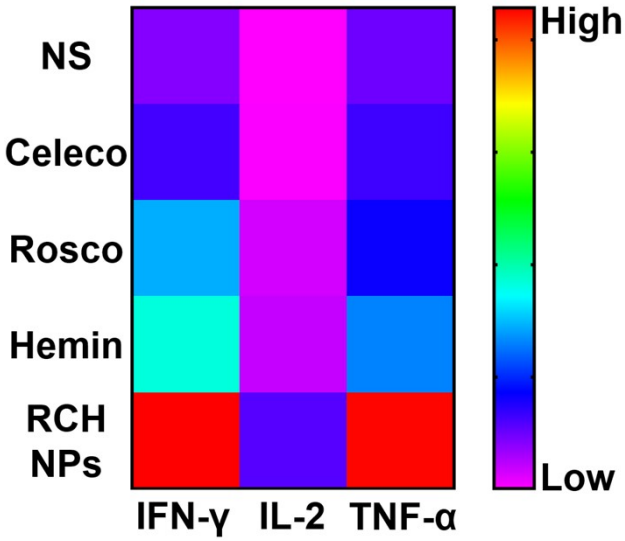

Fig. S14 The systemic cytokines secretion in the serum of mice.

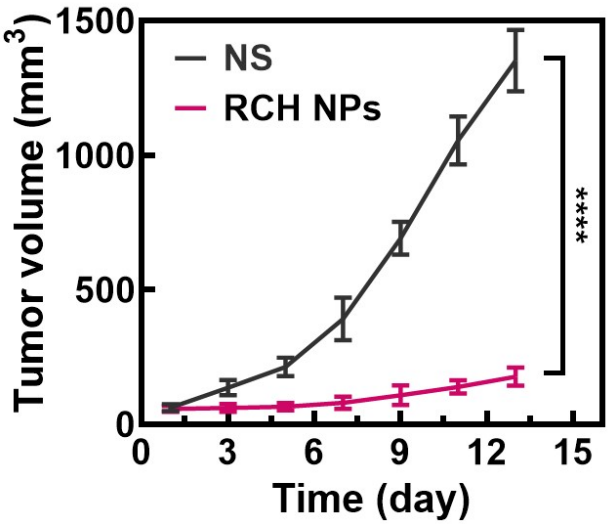

Fig. S15 Change in average primary tumor volume.

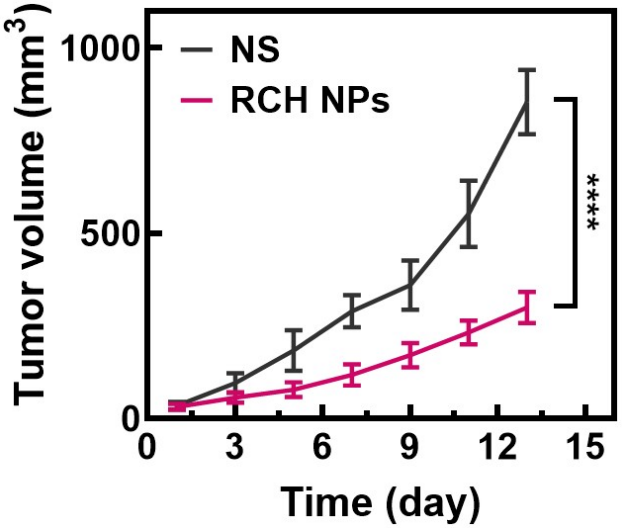

Fig. S16 Change in average abscopal tumor volume.

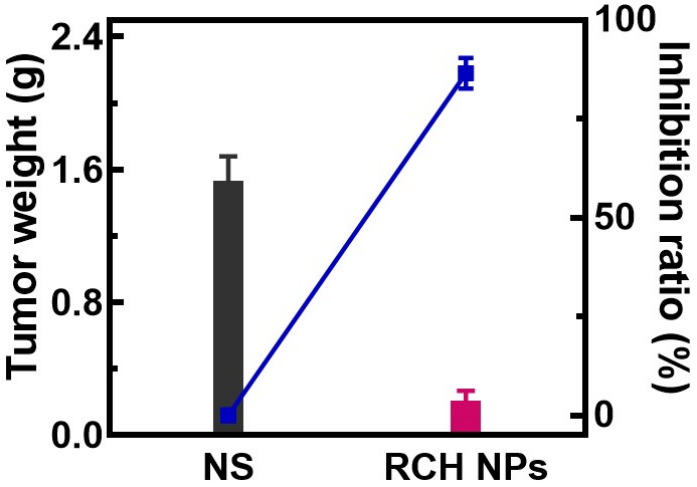

Fig. S17 Change in average primary tumor weight and tumor inhibition ratio.

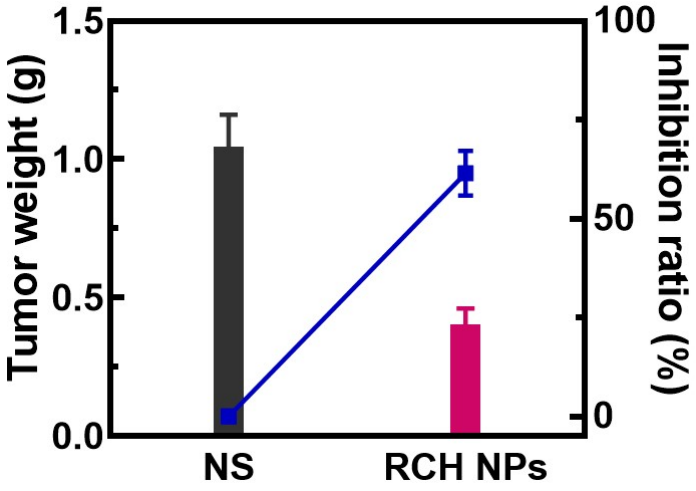

Fig. S18 Change in average abscopal tumor weight and tumor inhibition ratio.

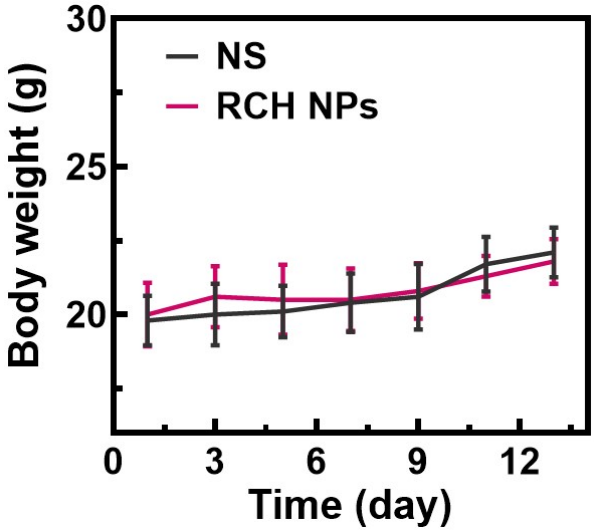

Fig. S19 Change in body weight of mice after different treatments in bilateral tumor model.

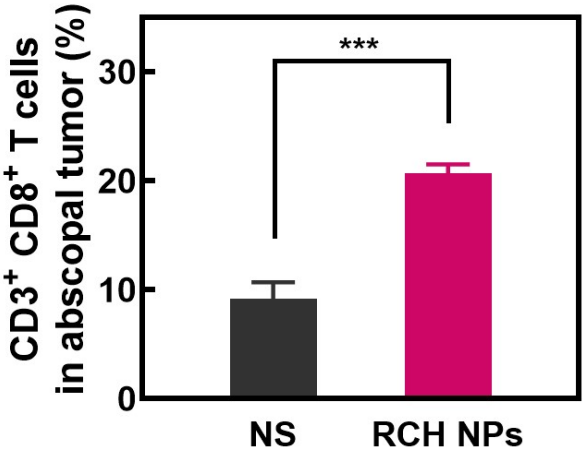

Fig. S20 Flow cytometry results of populations of CTLs in abscopal tumor of different groups.

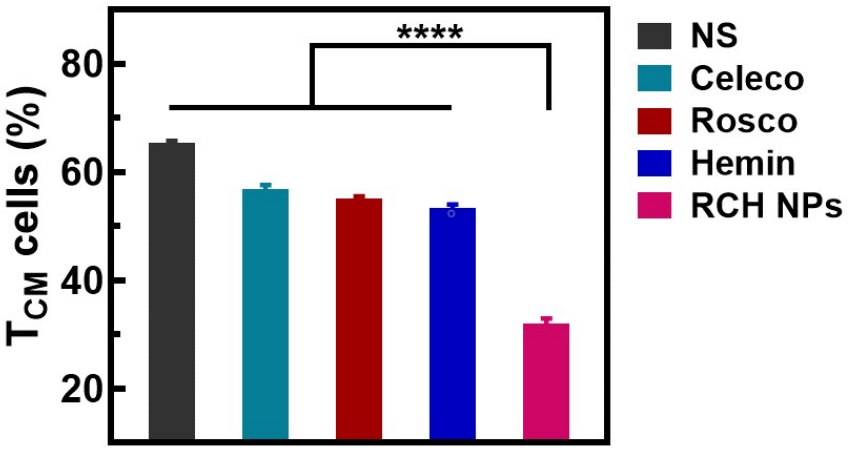

Fig. S21 The percentage of the central memory T cells in spleens from different treatment mice.

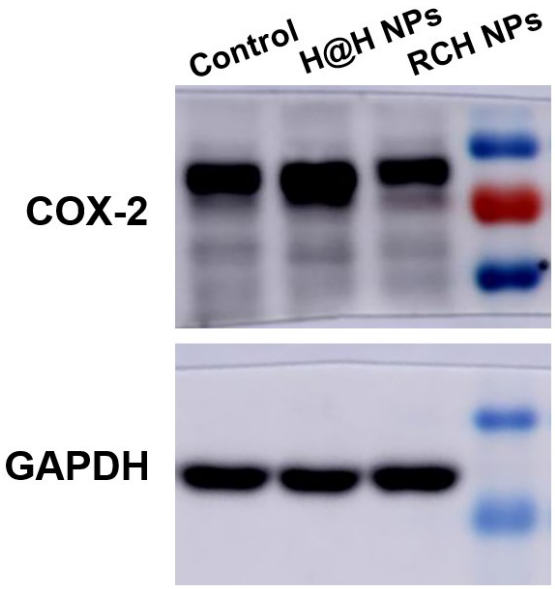

Fig. S22 Western blot images of COX-2 expression for different treatments.